

5.

The 1983 Liege Earthquake: Damage Distribution and Site Effects

D. Jongmans and M. Campillo

On November 8, 1983, a moderate magnitude ($M_L=4.9$) earthquake struck Liege (Belgium). A damage study has shown that site effects at different scales have played an important role in amplifying ground motion. On a large scale, the damage distribution has been determined by the presence of a large Carboniferous syncline beneath the city as shown by 2D numerical modeling. On a small scale, the main damage concentrations can be correlated with local superficial deposits which have amplified ground motions in the frequency range of buildings. A geophysical survey was carried out to measure the shear wave velocity of the different formations. Site response computations were made at numerous sites in order to estimate the possible amplification and to compare the results with the damage. It was shown that the spectral amplifications computed in the dominant frequency range of the buildings are consistent with the damage data. In very affected areas, 1D amplifications of 4 to 6 were obtained and in some cases 2D effects may have occurred.

The Liege earthquake, taking place in the intraplate region of Northwestern Europe, presents a significant interest to other similar areas as the eastern United States.

INTRODUCTION

On November 8, 1983 at 0h49m., an earthquake of magnitude $M_L=4.9$ and shallow depth occurred beneath the western suburb of Liege, Belgium (figure 1). This shock reached a maximum intensity of VII (M.S.K. scale) at the epicenter and was

(D J) Lab. de géologie de l'ingénieur, Liège University, Belgium
(M C) Observatoire de Grenoble, Université J. Fourier, France.

largely felt in Belgium, Germany and the Netherlands. This is the strongest earthquake in the area since the beginning of the century. The last main event was the Liege earthquake of December 21, 1965 with magnitude $M_L=4.5$.

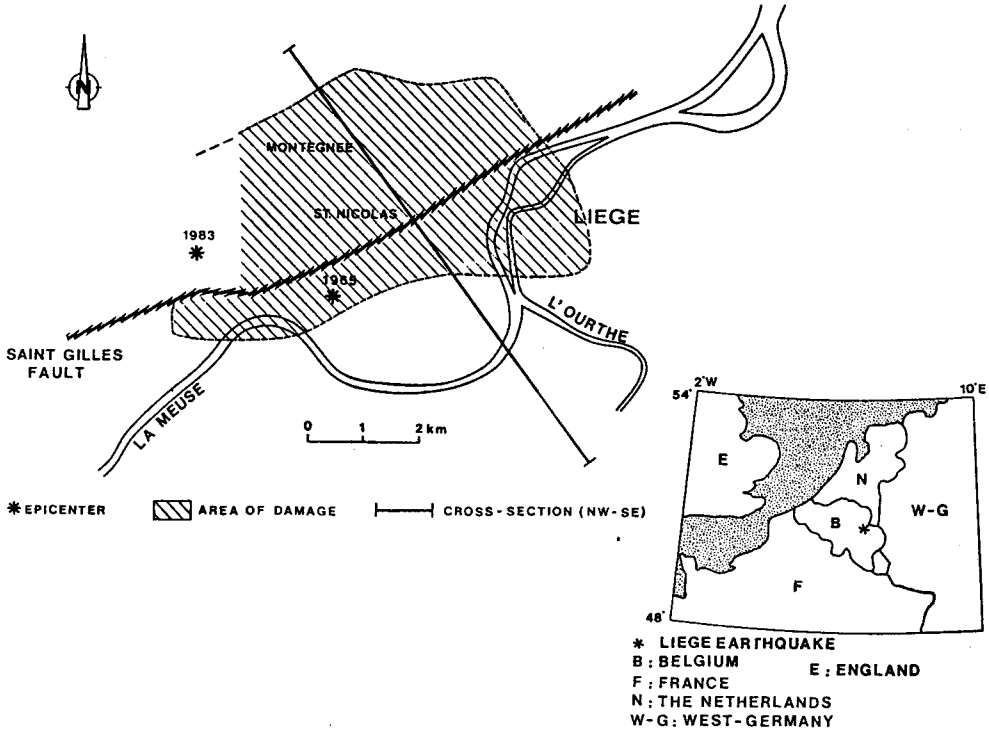


Figure 1 - Situation map and structural sketch-map of the Liege basin.

The November 8, 1983 earthquake was followed by a few aftershocks, the strongest of which had a magnitude of 3.4. When the earthquake occurred, the nearest seismological station was 35 km away from the epicenter. The hypocenter has been located with the data from 40 stations within the epicentral distance range of 500 km in Belgium, Germany, Luxembourg, The Netherlands, France and Great Britain. The hypocentral coordinates calculated by the Royal Observatory of Belgium (Camelbeeck and De Becker, 1985) are : latitude 50.63° N ± 0.6 km, longitude 5.50° E ± 0.8 km, depth 4 km ± 2 km. The instrumental epicenter locations of the 1965 and 1983 earthquakes are shown in figure 1 with the geological setting of the Liege area and the extension of the damaged zone.

Liege, a city of 400 thousands people, is located in the east of Belgium at the border of Germany and the Netherlands. The town is built in the alluvial plain of the river Meuse at its junction with the river Ourthe (figure 1). The suburbs are extending on the nearby hills. Liege is a typical city of western Europe for which an important part of the urbanization is the result of the industrial expansion of the 19th century. Its expansion has been founded on coal mines and steel industry. Liege has some quite striking similarities to many other industrial cities of N-W Europe likely to be affected by a moderate earthquake. A precise evaluation of the damage is interesting as a good example of what may occur in other parts of Europe and in the eastern United States.

GEOLOGICAL STRUCTURE

Liege lies on Devonian and Carboniferous formations belonging to a tectonic unit called the Namur synclinorium. To the north, this unit is discordant on the Cambro-Silurian basement (Brabant massif) whereas to the south it is limited by a great thrust fault called Eifel fault (figure 2). The stratigraphic section of the Namur synclinorium is :

- Westphalian shales and sandstones of about 1300 m thickness containing coal layers which have been worked for a long time. These rocks outcrop in the town
- Namurian shales and sandstones about 300 m thick
- Visean limestone 150 to 200 m thick
- Some thin layers of Frasnian, Givetian and Famennian ages.

These Paleozoic rocks are affected by a succession of NE-SW orientated folds (figure 2). In the north, the layers gently dip to the south and form the northern limb of a large syncline 8 km wide lying beneath the town. The southern limb is composed of a succession of small synclines and anticlines often overfolded. The syncline is followed to the south by the Chartreuse anticline and another syncline cut by the Eifel fault.

All the Carboniferous basin is affected by a set of longitudinal faults, trending northeast-southwest (figures 1 and 2). These faults generally dip steeply at angles between 45 degrees and vertical. They show important horizontal motions ranging from a few hundreds meters to one kilometer. The general motion is a displacement of the northern block to the east.

The epicenters of the 1965 and 1983 earthquakes are located near the surface trace of the St.Gilles fault that was recognized in the coal mines to be steeply dipping at depth. The hypocenter locations are therefore consistent with the fault geometry at depth.

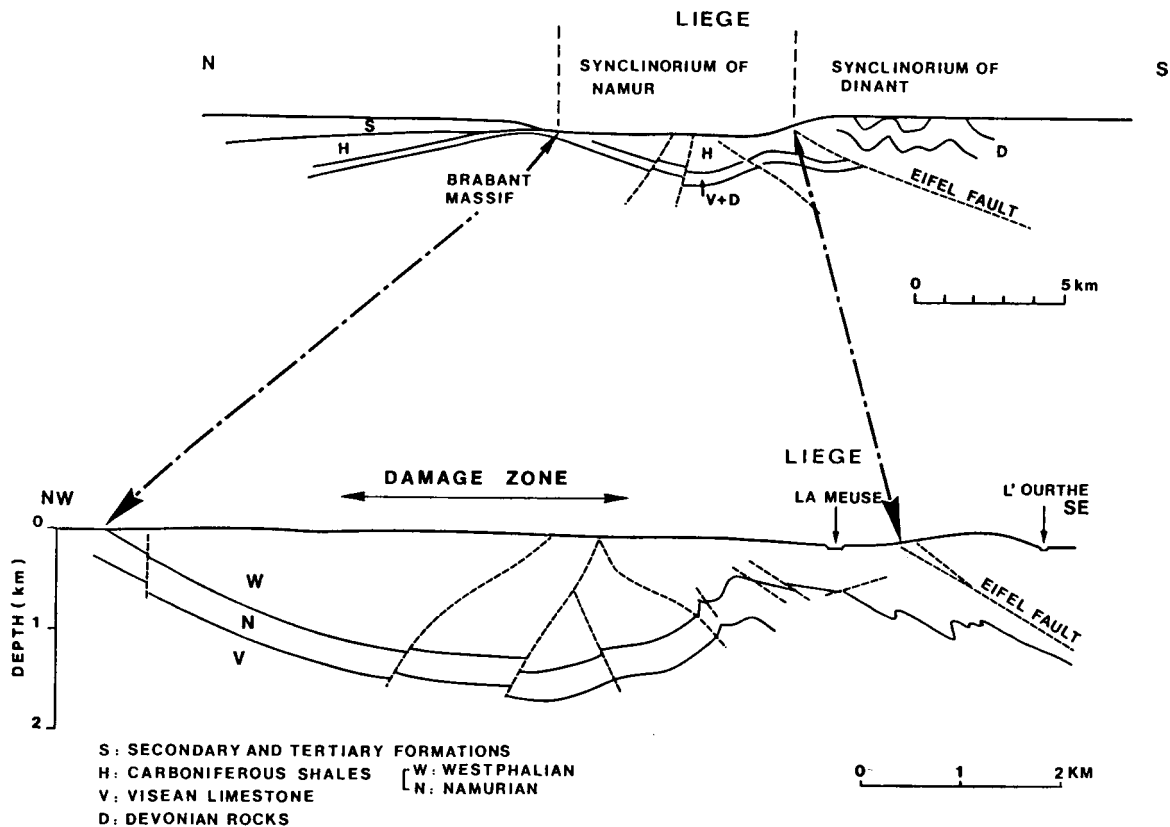


Figure 2 - Geological cross-section of the Liege area.

After the Variscan orogenesis, the Paleozoic rocks were eroded to a peneplain formation and covered by flat-layered Mesozoic and Cenozoic sediments. These layers are mainly exposed on the hillside in the north of Liege. Quaternary formations are composed of alluvial deposits, slope deposits and some terrace levels.

LARGE-SCALE EFFECT

Two fault plane solutions have been proposed from the P-wave first motion data of the 1983 Liege earthquake (Ahorner and Pelzing(1985), Bonjer and Faber(1985)). The first solution is a predominating strike-slip dislocation combined with a small thrust component, the other one being nearly a dip-slip with normal faulting. In both cases, the chosen fault plane has a roughly east-west trending and dips 60 to 80 degrees in a northerly direction. These features are consistent with the St.Gilles fault geometry.

On the other hand, the damage observations may help solving the ambiguity of the possible fault plane solution. A striking feature of the damage is indeed that, in the streets parallel to the St.Gilles fault, the façades moved perpendicularly to their plane, while in the perpendicular streets, the front walls were affected by shear cracking. This suggests a prominent ground motion perpendicular to the fault trace. For both focal mechanisms, Jongmans and Campillo (1989) have computed the surface accelerations generated by a double-couple point source located in a layered medium, using a numerical method developed by Bouchon (1981). It was shown that the strike-slip dislocation fits better with the surface motions deduced from building observations and that the damage pattern is consistent with the maximum horizontal computed motions.

The general pattern of the damage area is elongated NE-SW (see figure 1) with the higher intensity concentrated in the western part of the town and in the suburbs of St. Nicolas and Montegnée. This is also the strike of the syncline structure. Moreover, in the NW-SE direction, the damage is mainly located above the Carboniferous syncline (figures 1 and 2) which is a large structure likely to cause seismic waves amplification. This kind of phenomena has been observed for a long time in sedimentary basins. From field studies of great earthquakes, it is well established that sedimentary basins and alluvial valleys can experience surface motion amplification. Such effects have been numerically studied by different authors (for a complete review, see Sanchez-Sesma(1987) and Aki(1988)). For instance, Bard(1985) systematically investigated the seismic response of two-dimensional sediment-filled valleys to plane-incident waves using the method developed by Aki and Larner (1970). The assumed planarity of the incident wave front theoretically restricts

the results to distant earthquakes. On the contrary, the 1983 Liege earthquake occurred at shallow depth and the epicenter was located close to the affected area.

In order to take into account the source location, we have used a discretized form of boundary integral equations (Campillo, 1987). This technique allows the computation of synthetic SH seismograms in a laterally varying medium with plane and curved interfaces in the two-dimensional case. The diffracting interface is represented by an array of body forces located along the interface at equal spacing. The source can be located anywhere in the space. Propagation in flat layered zones is performed using the reflection-transmission method (Kennett, 1983).

For the calculations, the Carboniferous syncline has been assumed to have a sine shape and the surrounding half-space is overlaid with a thin low velocity layer. The geological configuration and the dynamic parameters used are given at the bottom of figure 3. Because of the moderate magnitude of the Liege earthquake, the extension of the source was neglected. Synthetic seismograms were computed at different points on the surface and the maximum spectral amplifications A_m are

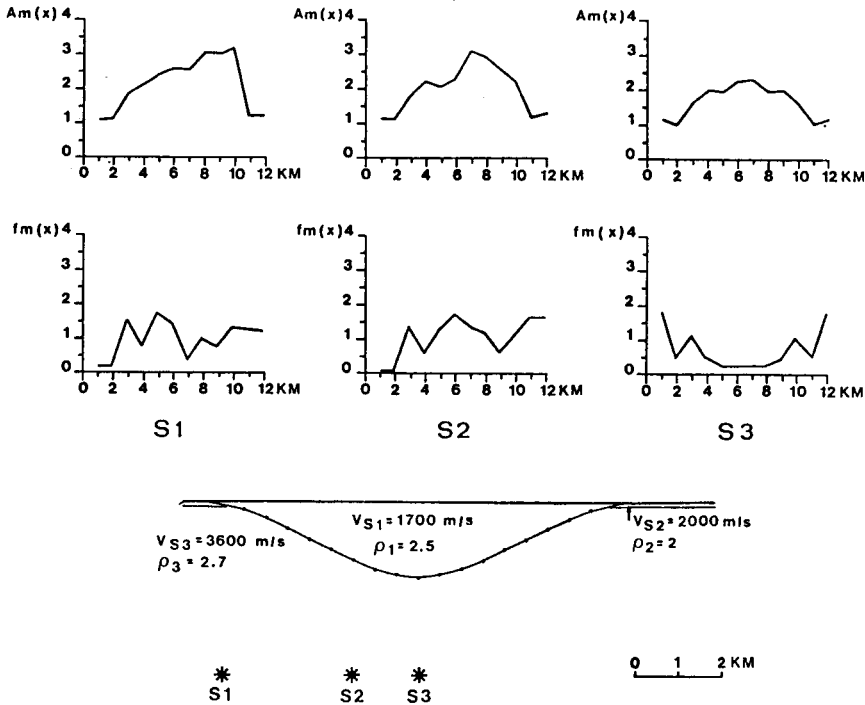


Figure 3 - Maximum spectral amplification for the sources S1-S2-S3

displayed on figure 3 (top) with the corresponding frequency fm for three source locations.

When the source is just below the syncline center, the maximum amplification (2.5) is obtained in the center of the structure for a frequency of about 0.25 Hz. If the source moves to the edge, the maximum amplification reaches higher values (3-3.5) and is located on the opposite site of the structure. According to the proposed hypocentral locations of the Liege earthquake, the idealized source would be between S1 and S2. The maximum amplification obtained in the center of the syncline is in good agreement with the location of the damage area. Other methods based on the assumption of incident plane waves were used. These methods include discrete plane wave representation (Aki and Larner, 1970) and the approximate ray technique of Sanchez-Sesma et al. (1988). The results obtained for the amplification are similar and indicate the validity of the plane wave assumption in this case (Jongmans and Campillo, 1989). The uncertainties due to the poor knowledge of the shear velocity structure are usually much larger than the discrepancies between these different theoretical approaches. In general, this affirmation has to be tempered because of effects due to the source extension that can be important in the near field for large earthquakes and because we restrict the analysis to SH waves in the 2D case.

GEOTECHNICAL ASPECTS

An interesting feature of the Liege area is the good knowledge of the geological configuration and of the mechanical properties of soils and rocks.

Rocks characteristics and geometry are known at depth from work mining, and near the surface from investigations for a tube project and for a tunnel site through the Carboniferous massif. Numerous geophysical studies, including cross-hole tests, seismic refraction profiles and well logging were carried out. The unconsolidated sediments mentioned above were investigated by a great number of bore-holes, cone penetration tests, laboratory tests and seismic refraction profiles including S-wave velocity determinations. Geotechnical maps covering the town (scale 1:5000) were compiled on the basis of all these data (Fagnoul et al., 1978). A simplified geotechnical map of the damaged area is presented in figure 4 . Two cross-sections along lines shown in figure 4 are given in figure 5 . P and S wave velocities for the formations were determined from refraction profiles performed at different locations along the cross-sections.

The different formations were divided into three main groups : bedrock, Secondary and Tertiary sediments, and recent deposits.

Carboniferous bedrock. It is composed of shales and sandstones including coal layers which have been worked for a long time. The mining has caused surface subsidence and has fractured the surrounding rocks. In-situ measurements at 20-30 m depth pointed out that static deformation modulus values could be divided by a factor of 5 in zones affected by the mining (Monjoie,1986).

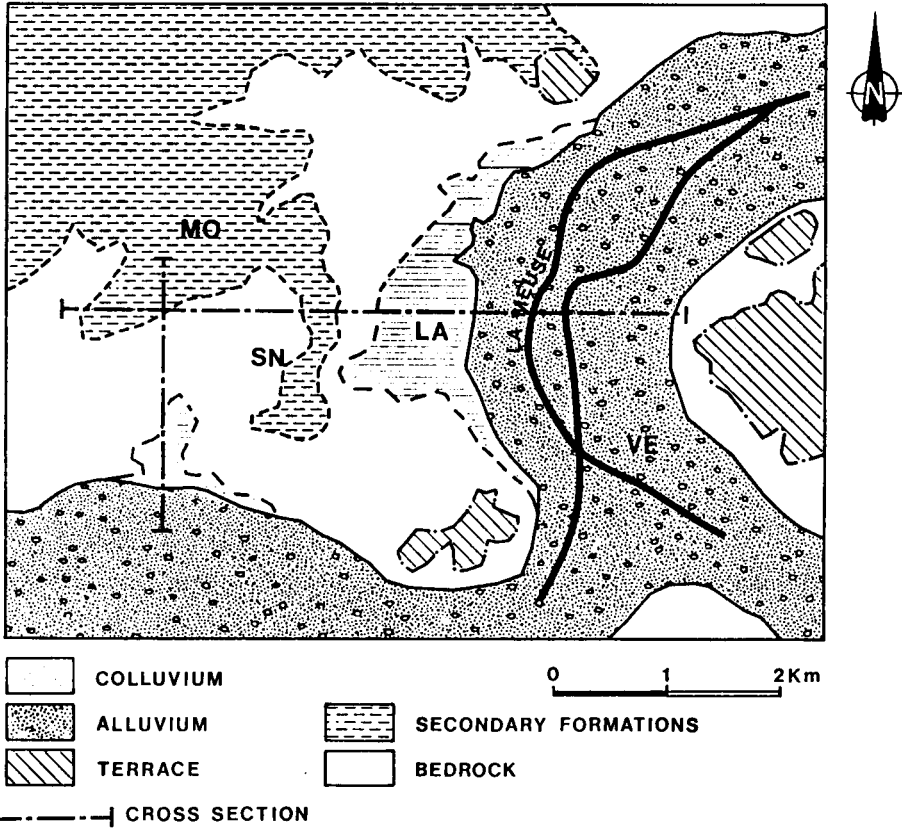


Figure 4 - Geotechnical map with the East-West and North-South cross-sections.

Typical velocity and density values in the Carboniferous massif are the following:

- in the weathered layer(10 m thick), $V_p=800$ m/s , $V_s=400$ m/s and $\rho =1.8$.
- between 10 m and 15 m, V_p , V_s and ρ increase to reach respectively 2500 m/s, 1250 m/s and 2.5 .
- at depth (more than 100 m deep), $V_p= 3500$ m/s, $V_s= 1750$ m/s and $\rho = 2.65$.

Secondary and Tertiary sediments. The Secondary deposits consist of a bed of greenish marly clay underlying a thick layer of chalk and dip slightly to the north-west.

The marly clay, a few meters to 10 meters thick, is characterized, according to USCS, as a clay of high plasticity. Its density ranges from 1.8 to 2.0 and the compression strength is about 5 MPa. The P-wave velocity

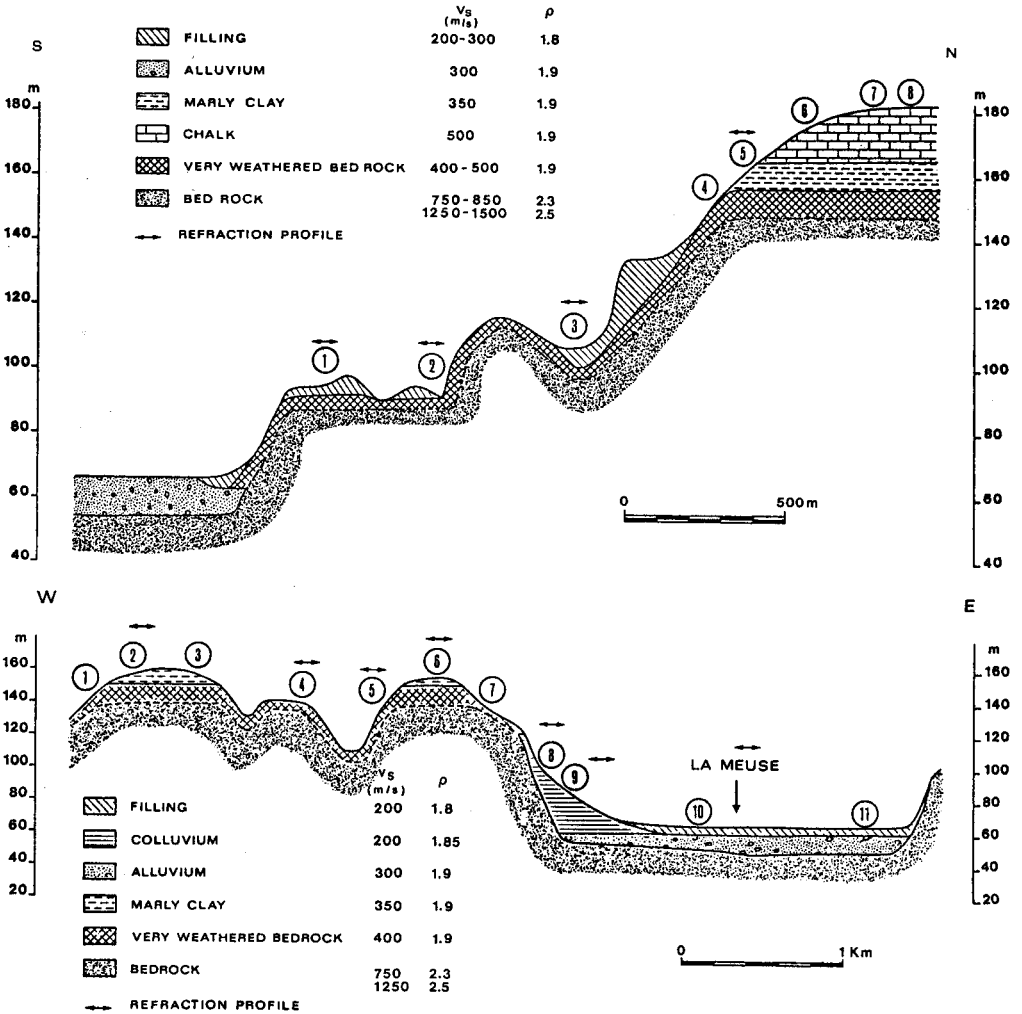


Figure 5 - Cross-sections along the two lines shown on Figure 4.

varies between 600 and 1000 m/s while the S-wave velocity ranges from 300 to 400 m/s.

The chalk, white to greyish, has a maximum thickness of 30 m. At the top of the layer, caverns may appear as a result of chalk solution by meteoric waters and are likely to cause damage to buildings. The compression strength ranges from 5 to 10 MPa while the density is about 1.9. The chalk is characterized by P-wave velocities from 1000 to 2500 m/s according to the consolidation degree. The S-wave velocity ranges from 500 to 750 m/s.

Recent deposits. They consist of alluvial deposits, slope deposits and fillings. The alluvial plain of the Meuse river, a few hundreds meters to one kilometer wide, consists mainly of a layer of gravel (5 to 10 meters thick) underlying silty sand. In some places, the deposits are however very heterogeneous and can be composed of clay and peat, especially at the junction of the Meuse and the Ourthe rivers. The total thickness of the alluvial deposits is between 12 and 15 meters. The P-wave velocity is highly variable, ranging from 300 m/s in silt and clay, to 1000-2000 m/s in saturated sand and gravel while the S-wave velocity varies between 100 and 400 m/s. The ground water level is generally found at the top of the gravel layer.

The slope deposits are encountered at the foot of the western hillside. They are made of fine-to-coarse grained soils such as silts, clay sands, sandy gravels and pebbles. In some places, these deposits reach an extension of a few hundreds meters and a maximum thickness of 30 to 40 meters. The density ranges from 1.6 to 2.0. They are characterized by a low P-wave velocity of about 400 to 500 m/s and a S-wave velocity as low as 200 m/s. Therefore, these deposits are very sensitive to seismic excitation.

As mentioned before, coal layers have been worked for a long time and old rock filling deposits are thus encountered here and there. The geometry and the location of these fillings are generally badly known. An example of a CPT test carried out in filling material is given in figure 6. P-wave velocity is about 300-500 m/s while S-wave velocity values of 200 m/s have been obtained. Another type of filling, consisting of construction materials remains and earth, is located mainly along the alluvial plain.

DAMAGE DISTRIBUTION

The general pattern of the area of damage is elongated NE-SW (see figure 1) with the higher intensity concentrated in the western part of the town and in the suburbs of St. Nicolas and Montegnée. About 13000 houses were more or less damaged. Of these, 25 were partially or totally destroyed. Two people

died during the earthquake and a few were wounded. During the days following the earthquake 4 people were killed by CO intoxication resulting of damage to chimneys. The repair cost was estimated to about 80 millions \$ but the real economic cost is higher.

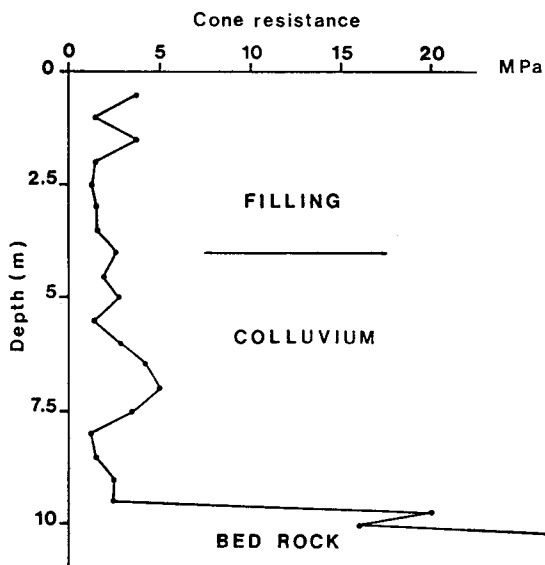


Figure 6 - Cone penetration test diagram.

As mentioned before, a maximum intensity of VII (MSK scale) was reached although some evidence may exist for locally higher intensities. Unfortunately, no strong motion accelerograms were recorded. The peak ground acceleration has however be estimated from field observations (Plumier, 1985 and Gurpinar, 1985). Motions of different structures and solids suggest that the horizontal peak acceleration reached 0.2 g in the epicentral area. The duration of the strong ground motion was limited to a few seconds.

In the affected area, the majority of the buildings are one or two story old masonry houses. The main characteristics of damaged buildings are listed in table 1.

The principal types of damage observed were :

- failure of chimneys (about 10,000). Fortunately, the earthquake occured during the night, at a time when people were not in the streets.
- vertical cracks between façade and cross-wall
- shear cracking in walls.

TABLE 1			
Main characteristics of damaged buildings			
Age	Percentage	Number of stories	Percentage
> 133 years	4 %		
133-109 years	6 %		
110-84 years	21 %	1	3 %
83-65 years	28 %	2	60 %
64-53 years	12 %	3	31 %
52-40 years	10 %	4 and more	6 %
39-20 years	12 %		
19-0 years	7 %		

In the affected area, the worst structural damage were confined to older and poorly built structures. Modern reinforced concrete buildings and well constructed brick built dwellings were generally unscathed. Photos illustrating the damage are presented in figures 7 to 9.

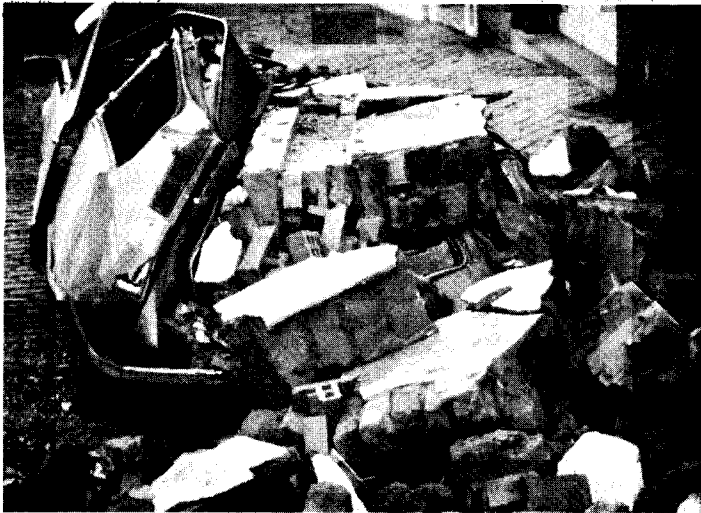


Figure 7 - Effect of chimney fall.

Our study was based on the examination of expert's reports concerning 9000 affected houses in Liege, St.Nicolas and Montegnée. These reports were established to meet indemnification requests from the owners of the damaged buildings. They comprise information on the damage observed and the repair costs.

A damage code was set up on this basis (see appendix 1). It consists of a gravity index for each of the following

damage types: failure of chimneys, cracks in interior and exterior walls, cracks in ceilings, fall of ornamental

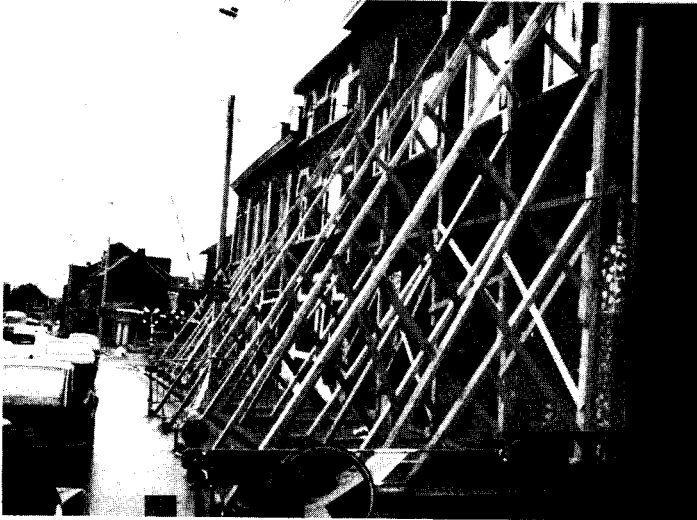


Figure 8 -
Displacement of
building front.

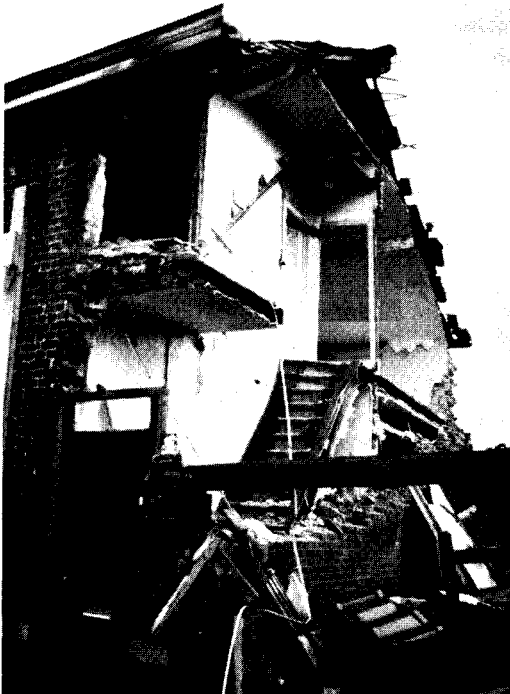


Figure 9 - Partially
collapsed masonry
building.

elements. On this basis, a damage index (id) was calculated for each building by a weighted sum of the gravity indexes that enhances the effect of the structural damages.

A file of 9000 records including the age, the number of

stories, the damage index and the location of the houses was created. The affected area was divided into squared meshes 200 m side. From the initial file, a second file concerning 804 meshes was computed. It includes for each mesh the number of damaged buildings (ndb), the total number of buildings (ntb), the number of stories distribution, the mean age of the buildings and different damage parameters. The following damage parameters were computed :

$$IDM = (\sum id) / ndb \quad (1)$$

$$IDP = (\sum id) / ntb \quad (2)$$

$$IDMP = (\sum id) / \sqrt{(ndb * ntb)} \quad (3)$$

The second parameter IDP takes into account the percentage of damaged buildings. High IDP values characterize areas where a great number of buildings were affected while high IDM values mark areas where buildings were strongly damaged whatever their number may be. In order to point out the areas where a great number of buildings were strongly affected, we have used the third parameter IDMP given above. The corresponding damage map is presented in figure 10.

In a similar way, a mean construction age map was obtained (figure 11). Comparing figures 10 and 11, it appears that the building age seems to have little influence on the damage distribution. Most of the ancient buildings are indeed located in the center of the town where no or weak damage concentration is shown. However, a small area with old houses appears in the west of Montegnee where significant damage were observed. This will be discussed further when we will compare the damage concentrations with the geotechnical map.

SMALL-SCALE EFFECT

As shown in figure 10, the damage are concentrated in some zones, the area of which ranges from a few hundreds to a few thousands square-meters. So far, we have studied the source and large-scale site effects without consideration for the detail of the damage distribution. The latter can only be explained by amplification effects due to soft superficial deposits.

Damage concentrations especially appear in the western part of the map (Montegnee area), at the foot of the western hill-side (LA) and in very localized areas in the alluvial plain (VE) .

The damage concentration at the foot of the hill side (zone LA) matches very well with the slope deposits location, the thickness of which can reach 30-40 m. In the western part of the map, damage is concentrated in the Montegnée area (MO)

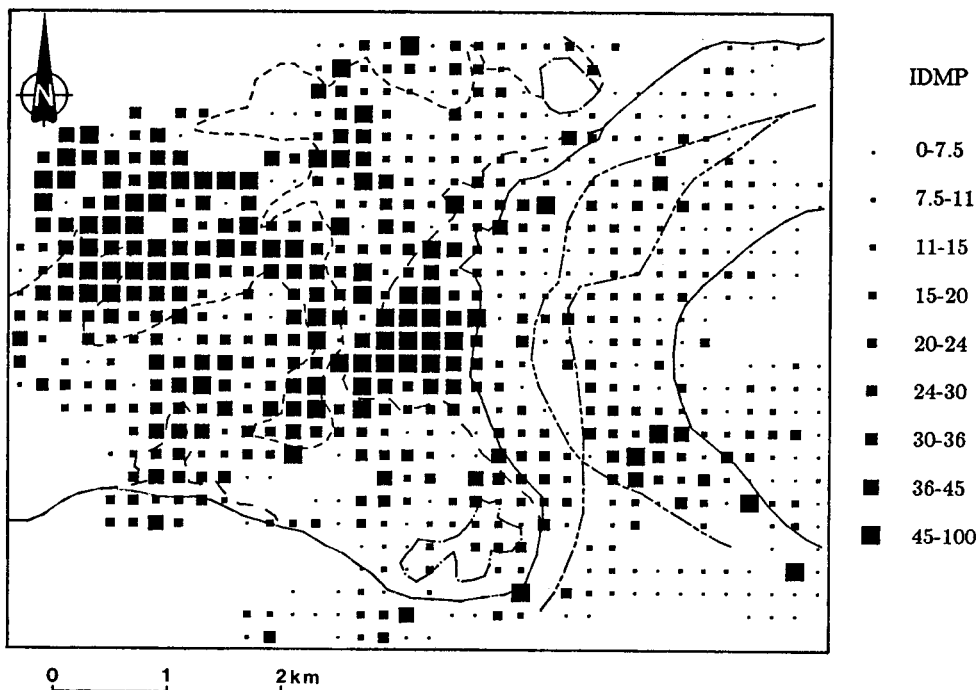


Figure 10: Damage map with geotechnical sketch map. The black squares represent equal occurrence classes of the damage index IDMP.

present. This correlation is also clearly seen in the east of St. Nicolas (SN) where a tongue of Secondary formation corresponds to a very damaged zone.

In the western part of St. Nicolas, where the bedrock outcrops, damage are more scattered and one can observe small-scale damage concentrations. However, as pointed out in section (4), recent deposits (colluvium and filling) are encountered here and there in this area. On the geotechnical map some of these deposits are shown, especially a dejection cone at the limit of the alluvial plain. The location and thickness of these formations are nevertheless generally very badly known. Penetration tests (figure 9) have revealed that houses could be built on 10 m soft deposits consisting of old filling and colluvium. Yet, these are likely to cause severe local motion amplifications.

In the alluvial plain, damage are less important and more scattered, except at the junction of the Meuse and the Ourthe (VE on figure 4) where a damage spot clearly appears. This area is characterized by the presence of ancient arms of the river and of very heterogeneous alluvial deposits.

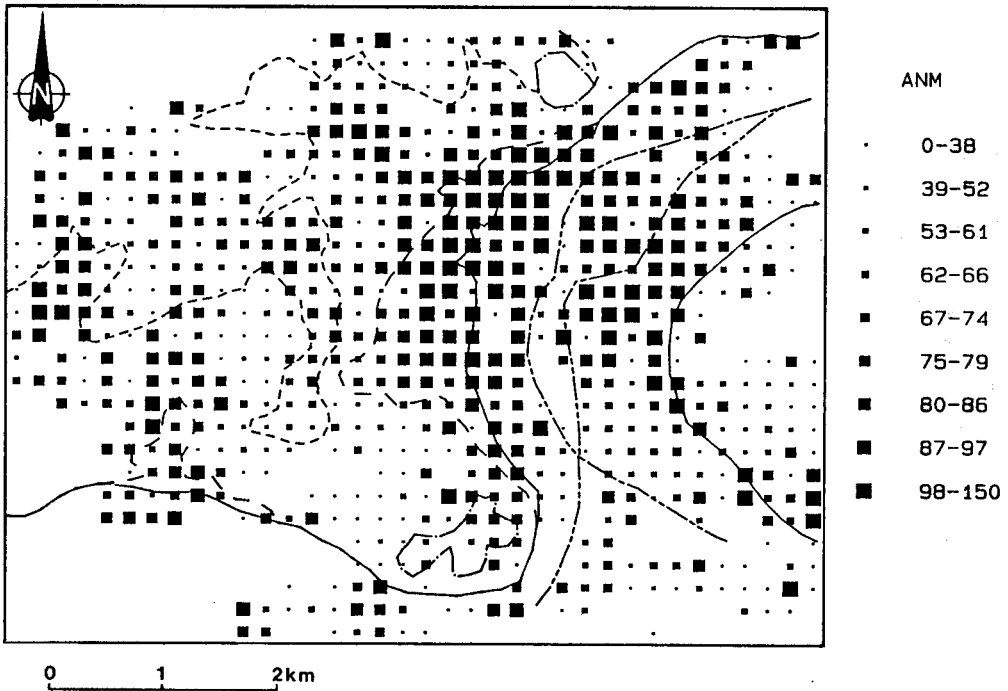


Figure 11: Mean building age map. The black squares represent equal occurrence classes of the age.

From these observations, it appears clearly that the main damage concentrations are correlated with the presence of soft superficial deposits overlying the Carboniferous bedrock. In order to interpret these observations, we have computed site amplifications on the basis of the geological and geophysical characteristics given in section (4). With this aim, two kinds of models have been used. The first is a one-dimensional plane layer model (1D) and the second includes two-dimensional heterogeneity (2D).

1D model

The elastic Fourier transfer functions of plane layers have been computed at different points along two cross-sections. The first one, orientated East-West (figures 4 and 5) goes through the alluvial plain, the slope deposit and the Secondary formations exposed on the top of the topography (St. Nicolas). The second cross-section is South-North (figures 4 and 5) and goes from the alluvial plain to Montegnée. The density and velocity values used for the computations are given in figure 5. The calculations were performed with two sets of values of quality factors. In the

first case, we have assumed Q_s to be 1000 for soils and rocks. In the second case, we have considered higher attenuation values: $Q_s=20$ for soils and $Q_s=100$ for Carboniferous

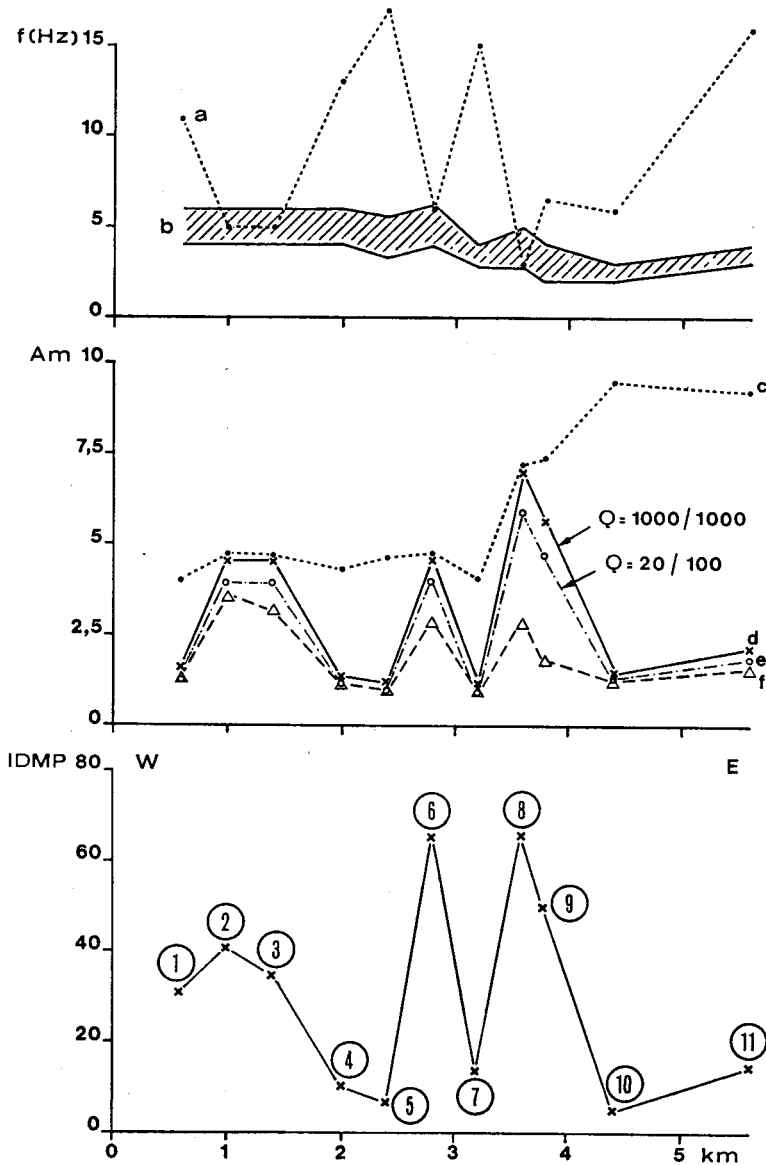


Figure 12 - Up: Frequency of maximum 1D amplification and mean value of the natural frequency of building along E-W cross-section. Middle: Amplification curves (see text for description). Bottom: Damage parameter. The horizontal scale is the same for all curves.

formations, which are more realistic from our experience of these materials in the Liege area. The horizontal plane layers response to vertically incident SH-waves was computed with a maximum frequency of 25 Hz.

Our results are presented on figures 12 and 13 where they are compared with the observed damage parameter curves (lower parts of the figures). We have shown the parameter IDMP but the curves obtained with IDM or IDP are similar. The upper parts of the figures present the frequencies for which the maximum amplifications are occurring for the 1D-models (curve a). On the same graphs are drawn the mean values of the natural frequencies of the buildings (curves b). The dominant frequency of buildings F_0 (in Hz) can be roughly given by the approximate relation :

$$F_0 = 10/N \quad (4)$$

where N is the number of stories

For each mesh, we calculated the mean value of the natural period F_m .

In the middle of the figure four spectral amplification curves along the cross-sections are presented. The first one (c) corresponds to the maximum of the elastic amplification from 0 to 25 Hz, while the others take into account the natural frequency of the damaged buildings. The curves (d) and (e) on figures 12 and 13 represent the maximum possible amplification in the range $(T_m-0.05, T_m+0.05)$ computed for the two models of quality factor considered. For drawing the curve (f), we computed the elastic seismic response corresponding to each class of number of stories. On this basis, the total spectral amplification of the mesh was obtained by the average of the different amplifications, weighted by the percentage of each class of buildings.

E-W cross-section (Figure 12). It shows that the maximum amplification curve (c) doesn't succeed in explaining the damage evolution, especially in the alluvial plain where very high amplifications ($A_m=9$ in the elastic domain) are expected but in a frequency range very different from the frequency of the buildings. On the contrary, amplification curves (d) and (e) are well correlated with the damage curve. The 1D model does predict the relative high amplification in the slope deposit ($A_m=6-7$), the peaks corresponding to the calcareous clay localizations ($A_m=3.8-4.5$) and the low amplification in the alluvial plain. The highest amplifications are obtained when the frequency giving the maximum amplification falls into the frequency range of the buildings (see the top of figure 9). Curve (f) shows the same variations than the preceding ones. One can nevertheless observe the relatively lower amplifications obtained on the slope deposit and on the nearest calcareous clay layer. These results, compared to the

damage, suggest possible 2D effects at these sites.

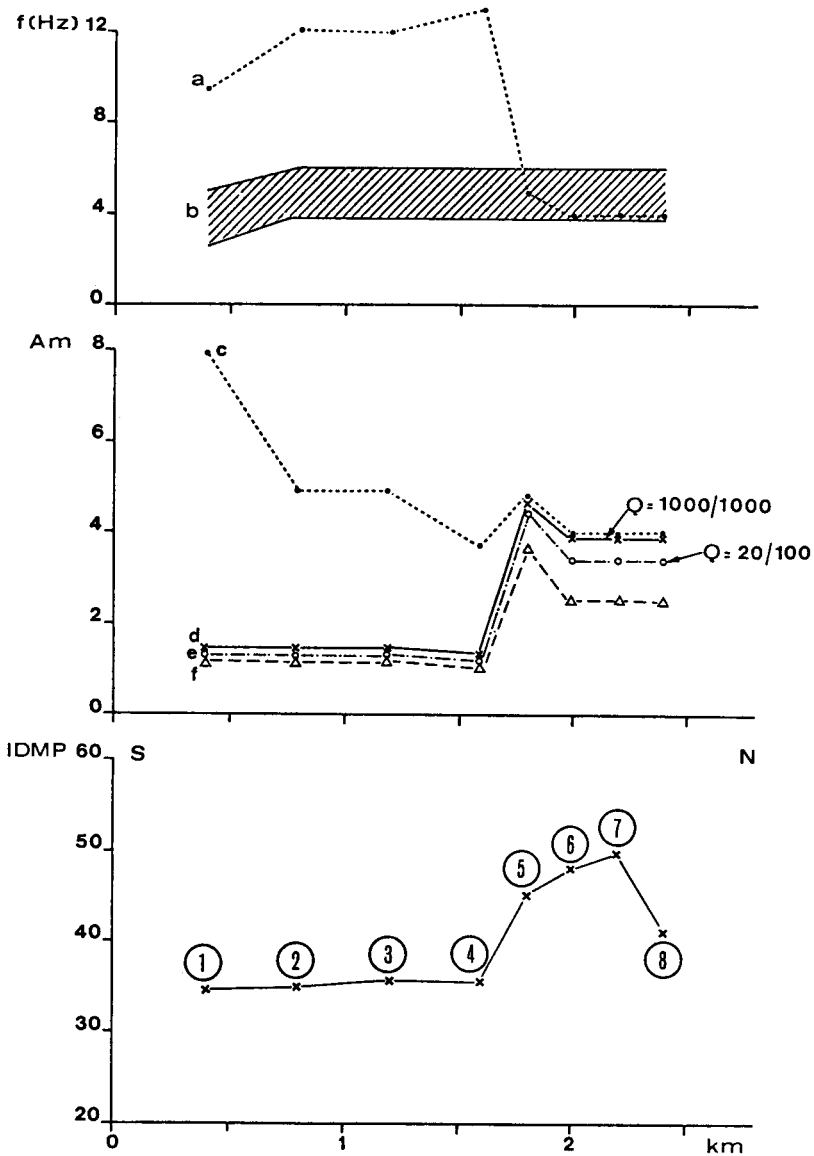


Figure 13 - Up: Frequency of maximum 1D amplification and mean value of the natural frequency of building along N-S cross-section. Middle: Amplification curves (see text for description). Bottom: Damage parameter. The horizontal scale is the same for all curves.

N-S cross-section (Figure 13). As along the other cross-section, amplification curve (c) doesn't explain the damage distribution. On the other hand, curves d and e

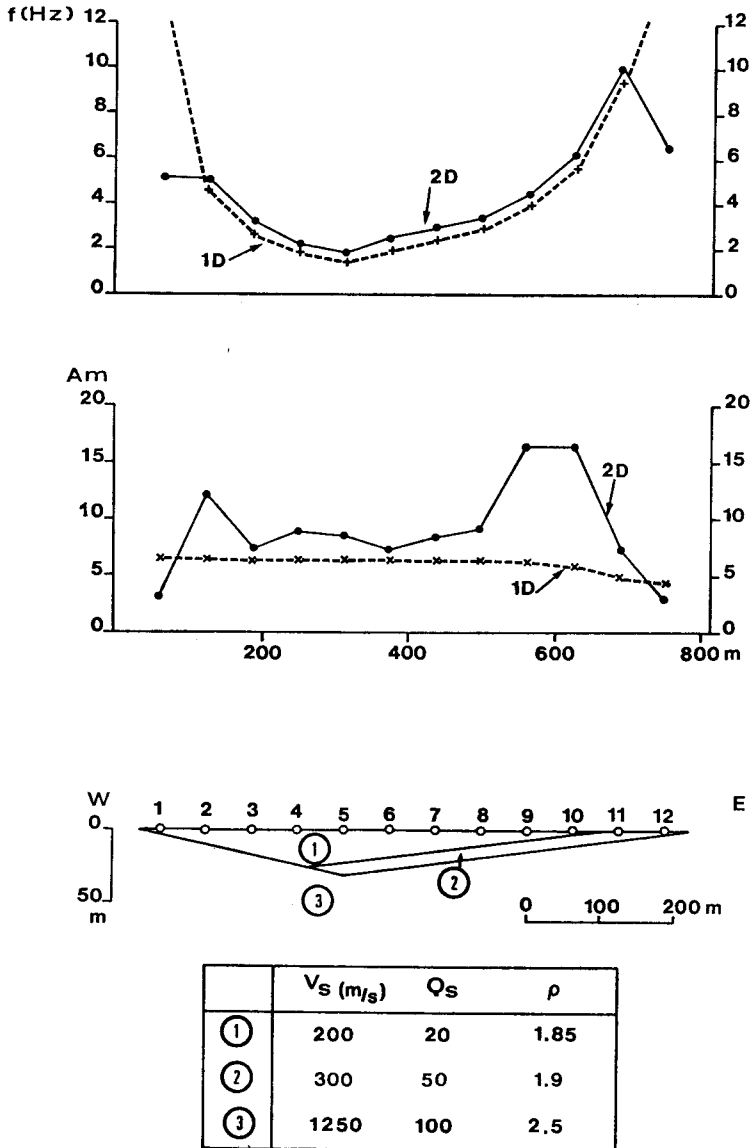


Figure 14 - Comparison between 1D and 2D responses to vertically incident plane wave. *Up*: Frequency of maximum amplification. *Middle*: Maximum amplification curves. *Bottom*: Configuration used.

succeed in predicting the damage increase on the Secondary formations. With realistic Q values, maximum amplifications of 3.4 to 4.4 were computed for a frequency of about 4-6 Hz.

2D model

The 1D model used above, although it explains the main features of the damage pattern, is not able to take into account effects due to the finite lateral extent of superficial deposits. This generally tends to increase the amplitude and the duration of the ground motion. Figure 5 indicates that the slope deposit at the foot of the hill-side has a lateral extension likely to generate surface waves. We have computed the response of the structure with the Aki-Larner method (Aki and Larner, 1970) in its extension for multi-layered media (Geli et al., 1988). The geometry and the dynamic characteristics used for the modeling are displayed at the bottom of figure 14. The spectral amplification curve, also presented in figure 14, show that in the central part of the deposit the amplification is about 7 to 9 for a frequency ranging from 2 to 3 Hz. These values are 30 to 50% higher than the values computed in the 1D case using the same dynamics parameters (figure 14). This result illustrates the influence of the 2D effect on the deposit response. In the Liege area, the slope deposit seems to be the only superficial structure likely to generate such effects. At the edges of the deposit, amplifications can reach values as high as 22 in the frequency range 4-6 Hz. However, these results probably overestimate the actual effect. As one can see in figure 5, the deposit is open at its edges and cannot trap all the energy.

CONCLUSIONS

The Liege earthquake of November 8, 1983 (ML=4.9) is the kind of event likely to affect any town in the western part of Europe and in the eastern United States. The relatively important damage observed are due in part to the poor quality of the old masonry buildings. On the other hand, this study has shown that site effects at different scales have played a significant role in amplifying ground motion.

On a large scale, the damage distribution seems to have been determined by the presence of a large Carboniferous syncline under the town. 2D modeling computations have shown that spectral amplifications of about 3-4 could have occurred in the affected area. However, these effects are not sufficient to explain the "hotspots" appearing on the damage map. Our study has pointed out that the main damage concentrations could be correlated with local geological structures such as slope deposits and horizontal soil layers overlying the Carboniferous bedrock. With 1D modeling, maximum spectral amplifications of 4 to 6 have been computed in the dominant frequency range of buildings. Moreover, when

the superficial formations are laterally confined (slope deposits) spectral amplifications as high as 9 can be reached in the same frequency range. This is a two-dimensional effect.

The example of the Liege earthquake illustrates the importance of the conjugate influence of geological structures at different scales on the damage intensity and spatial pattern. Such effects were already pointed out by Bard et al. (1988) in their study of the great Michoacan earthquake of 1985. Clear evidences have been presented of significant amplifications in Liege. They take place at relatively high frequencies and appear associated with well identified superficial structures.

ACKNOWLEDGMENTS

We thank A. Monjoie and the several people from L.G.I.H. (Liege University) who make available the damage data we used in this work. A. Plumier kindly provides us the photographs. We have appreciated the valuable comments of F. Sanchez-Sesma.

APPENDIX 1 Damage code by dwelling

Affected part	Damage description	gravity index
Chimneys	- No damage	0
	- Chimneys broken	1
Roofing	- No damage	0
	- Slight damage	1
	. replacement of less than 50 tiles	
	. shoring in the storehouse on an area less than 15 square metres	
	. battens to repara	
	. dormer-window broken	
	- Heavy damage	3
	. replacement of more than 50 tiles	
	. shoring in the storehouse on an area more than 15 square metres	

Affected part	Damage description	gravity index
Interior walls	<ul style="list-style-type: none"> - No damage - Slight damage <ul style="list-style-type: none"> . cracked plaster . less than 1.5 cubic metres masonry to repair - Heavy damage <ul style="list-style-type: none"> . more than 1.5 cubic metres masonry to repair 	<ul style="list-style-type: none"> 0 1 3
Exterior walls	<ul style="list-style-type: none"> - No damage - Slight damage <ul style="list-style-type: none"> . cracks . mortar joints to repair . replacement of less than 50 bricks . less than 5 cubic metres to repair . shoring less than 20 square metres - Heavy damage <ul style="list-style-type: none"> . replacement of more than 50 bricks . more than 5 cubic metres to repair . shoring more than 20 square metres . setting reinforced concrete 	<ul style="list-style-type: none"> 0 2 4
Ceiling Flooring	<ul style="list-style-type: none"> - No damage - Slight damage <ul style="list-style-type: none"> . replacement of pavement . ceiling cracks - Heavy damage <ul style="list-style-type: none"> . demolition and reconstruction of flooring . shoring of ceiling 	<ul style="list-style-type: none"> 0 1 3
Decorative and brittle parts	<ul style="list-style-type: none"> - No damage - Slight damage <ul style="list-style-type: none"> . windows broken . doors, windows, building-stones, chimney pieces to take down and remount. - Heavy damage <ul style="list-style-type: none"> . replacement of stone window-frames . replacement of chimney pieces, lintels,... 	<ul style="list-style-type: none"> 0 1 2

References

- Ahorner L. and Pelzing R., 1985. The source characteristics of the Liege earthquake on November 8, 1983, from digital recordings in West Germany. In : Melchior Ed., Seismic activity in Western Europe - NATO ASI Series, Dordrecht, Vol. 144, 249-262.
- Aki K. and Larner L., 1970. Surface motion of a layered medium having an irregular interface due to incident plane SH-waves, J. Geophys. Res., 70, 933-954.
- Aki K., 1988. Local site effects on strong ground motion. "Earthquake Engineering and soil dynamics II - Recent Advances in ground motion evaluation", June 27-30, 1988, Park City, Utah.
- Bard P.-Y. and Bouchon M., 1985. The two-dimensional resonance of sediment-filled valleys, Bull. Seism. Soc. Am., 85, 519-541.
- Bard P.-Y., Campillo M., Chavez-Garcia F.J. and Sanchez-Sesma F.J., 1988. The Mexico Earthquake of September 19, 1985 - A theoretical investigation of large- and small-scale amplification effects in the Mexico City valley, Earthquake Spectra, August 1988, vol.4, number 3, 609-633.
- Bonjer K.-P. and Faber S., 1985. Phase recognition and interpretation at regional distances from the Liege event of November 8, 1983. In : Melchior Ed., Seismic activity in Western Europe - NATO ASI Series, Dordrecht, Vol. 144, 233-249.
- Bouchon M., 1981. A simple method to calculate Green's functions for elastic layered media, Bull. Seism. Soc. Am. 71, 959-971.
- Camelbeeck T. and De Becker M., 1985. The earthquakes of Liege of November 8, 1983 and December 21, 1965. In : Melchior Ed., Seismic activity in Western Europe - NATO ASI Series, Dordrecht, Vol.144, 223-233.
- Campillo M., 1987. Modeling of SH-waves propagation in irregularly layered medium. Application to seismic profiles near a Dome. Geoph.Prosp., 35, 236-249.
- Fagnoul et al., 1978. Carte géotechnique 42.6.3 Liège, Institut géotechnique de l'état et Centre national de recherches des constructions civiles, Bruxelles.

topography on earthquake ground motion: a review and new results, Bull. Seism. Soc. Am., vol. 78, 42-63.

Gürpınar A., 1985, Engineering implications of the november 1983 Liege earthquake, Annales des Travaux Publics de Belgique, n°4, 354-359.

Jongmans D. and Campillo M., 1989. Influence de la source et de la structure géologique sur la répartition des dégâts lors du tremblement de terre de Liège du 8 novembre 1983. Bull. Soc. Géol. de France, (8), t.V, 4, pp.849-857.

Monjoie A., 1986. Le tremblement de terre de Liège du 8 novembre 1983 - Influence de la géologie sur l'ampleur des dégâts. Association française de génie parasismique. Premier colloque national, 29-31 janvier 1986, Saint-Rémy lès Chevreuse, vol. I, 2/43-2/51.

Plumier A., 1985, Le séisme de Liège et ses implications pratiques, les effets sur les constructions, Annales des Travaux Publics de Belgique, n°4, 346-353.

Sanchez-Sesma F.J., 1987. Site effects in strong ground motion. Soil Dyn. Earthq. Eng., 6, 124-132.

Sanchez-Sesma, F.J., F.J. Chavez-Garcia and M. Bravo 1988. Seismic response of a class of alluvial valleys for incident SH waves. Bull. Seism. Soc. Am., 78, 83-95.